

# High-Quality Single-Layer Graphene via Reparative Reduction of Graphene Oxide

Boya Dai<sup>1</sup>, Lei Fu<sup>1</sup> (✉), Lei Liao<sup>1</sup>, Nan Liu<sup>1</sup>, Kai Yan<sup>1</sup>, Yongsheng Chen<sup>2</sup>, and Zhongfan Liu<sup>1</sup> (✉)

<sup>1</sup> Center for Nanochemistry, Beijing National Laboratory for Molecular Sciences, State Key Laboratory for Structural Chemistry of Unstable and Stable Species, College of Chemistry and Molecular Engineering, Peking University, Beijing, 100871, China

<sup>2</sup> College of Chemistry, Nankai University, Tianjin, 300071, China

Received: 30 October 2010 / Revised: 25 December 2010 / Accepted: 27 December 2010

© Tsinghua University Press and Springer-Verlag Berlin Heidelberg 2011

## ABSTRACT

Reduction of graphene oxide (GO) is a promising low-cost synthetic approach to bulk graphene, which offers an accessible route to transparent conducting films and flexible electronics. Unfortunately, the release of oxygen-containing functional groups inevitably leaves behind vacancies and topological defects on the reduced GO sheet, and its low electrical conductivity hinders the development of practical applications. Here, we present a strategy for real-time repair of the newborn vacancies with carbon radicals produced by thermal decomposition of a suitable precursor. The sheet conductivity of thus-obtained single-layer graphene was raised more than six-fold to 350–410 S/cm (whilst retaining >96% transparency). X-ray photoelectron spectroscopy (XPS) and Raman spectroscopy revealed that the conductivity enhancement can be attributed to the formation of additional sp<sup>2</sup>-C structures. This method provides a simple and efficient process for obtaining highly conductive transparent graphene films.

## KEYWORDS

Graphene, graphene oxide, reparative reduction, transparent flexible electrode

Owing to its excellent optical transparency and electrical conductivity, graphene film is a good candidate for transparent electrodes [1]. Moreover, graphene has been incorporated as a new building block in composite materials for a wide range of applications [2], taking advantage of its thermal stability and exceptional mechanical properties. All these promising applications require a large quantity of high-quality graphene with sufficient structural homogeneity over large areas. However, none of the reported methods can meet all the requirements. For example, the mechanical cleavage method yields only small graphene pieces and is not considered as

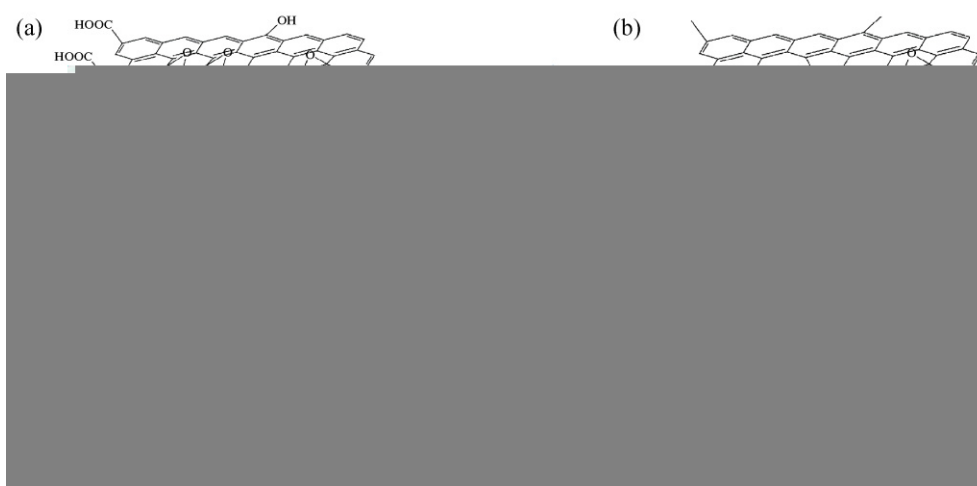
a scalable technique [3]. Another route involving epitaxial growth on expensive single crystal substrates needs ultrahigh vacuum which limits its practical applicability [4]. Rapid advances in chemical vapor deposition (CVD) of graphene have been achieved recently. However, unacceptable uniformity of Ni-CVD [5] and self-limited monolayer formation of Cu-CVD [6] create barriers to graphene electronics. Solution processes, such as organic synthesis [7], exfoliation of intercalated graphite in organic solvents [8], and chemical conversion from graphene oxide (GO) [9, 10] are predominant in massive production and cost-effective electronics.

Address correspondence to Lei Fu, leifu@pku.edu.cn; Zhongfan Liu, zfliu@pku.edu.cn

Because of the small lateral size of the resulting graphene and the low yield, both organic synthesis and intercalation–exfoliation have received much less attention than reduction of GO. GO is commonly obtained by oxidizing graphite powder in the presence of strong acids and oxidants. The sheet is decorated with hydroxyl and epoxy groups and carbonyl and carboxyl groups are attached at the edges [11] (Scheme 1(a)). These oxygen-containing functional groups disrupt the aromatic regions in the basal plane, so that the layer of GO consists of both aromatic regions and oxidized aliphatic six-membered rings, which leads to distorted  $sp^3$ -hybridized geometry and results in the insulating property of GO. Removing these oxygen-containing groups tends to restore the electrical conductivity of graphene. Typically, chemical reduction converts the insulating GO into sheets with up to four orders of magnitude higher electrical conductivity [12, 13]. However, either reducing GO in solution using reductants, for example, the widely applied hydrazine [9], or via thermal annealing [10], inevitably leads to the resulting reduced graphene oxide (r-GO) containing both lattice defects originating from the leaving or substitution of oxygen-containing groups and residual oxidized groups that are difficult to remove (Scheme 1(b)), which reduces the electrical conductivity. For monolayers of r-GO, electrical conductivities of only 0.05–2 S/cm have been reported,

which is less required for transparent electrodes [12]. Additionally, the defects and decorated oxygen may deprive the r-GO of some of the intrinsic properties of pristine graphene. Therefore, in order to exploit the macro-scale yield of the GO reduction approach, it is essential to find a strategy to restore the defective areas of graphene and improve its electrical conductivity.

Recently, López and colleagues used ethylene to heal reduced GO [14]. In their work, a GO sample was first reduced by thermal annealing in  $H_2/Ar$  mixture flow, and was then subjected to a carbon source. During the high-temperature thermal treatment, the epoxy groups or hydroxyl groups carried away the adjacent carbon atoms to form carbon oxides, which inevitably leaves behind lattice vacancies, leading to defective graphene structures [11]. As a result, they still detected a significant content of residual defects in their healed samples. Herein we present a more facile method to obtain high-quality graphene films by reparative reduction of GO in one step. When the oxygen-containing groups are just leaving, there remain the adjacent carbon atoms with dangling bonds. Then we have an opportunity to add extraneous carbon radicals into the sites (Scheme 1(c)) to form a relatively intact structure (Scheme 1(d)). The recovery of an ordered graphene structure was realized by introducing carbon radicals in the thermal annealing process via a rapid-heating process.



**Scheme 1** Structure of GO (a) and thermally reduced GO (b); Simultaneous reduction of GO and recovery of graphene structure (c), to obtain near pristine graphene (d)

GO was synthesized from natural graphite powder by a modified Hummers method [15, 16]. As-synthesized GO was treated by dialysis to completely remove residual salts and acids, and then dispersed in water under sonication to give a brown dispersion. The resulting dispersion was subjected to 10 min of centrifugation at 6700 rpm to remove unexfoliated GO. Single- to bi-layer GO films were fabricated by spin-coating of 1 mg/mL GO aqueous solution on hydrophilic substrates at 800 and 1600 rpm in sequence. The SiO<sub>2</sub>/Si and quartz substrates were first cleaned in piranha solution (7:3 H<sub>2</sub>SO<sub>4</sub>:H<sub>2</sub>O<sub>2</sub>) for 30 min at 90 °C, followed by rinsing with deionized water, then treated in RCA solution (5:1:1 NH<sub>3</sub>:H<sub>2</sub>O:H<sub>2</sub>O<sub>2</sub>:H<sub>2</sub>O) for 20 min at 90 °C, which was also followed by rinsing with deionized water. Finally the substrates were dried under an ultrapure nitrogen stream.

According to the tapping mode height images of atomic force microscopy (AFM), a fully-covered single- to bi-layer GO film can be obtained on SiO<sub>2</sub>/Si substrates. The single-layer GO sheets were ~1.1 nm in height (Fig. S-1 in the Electronic Supplementary Material (ESM)) and their lateral sizes ranged from several hundreds of nanometers to several micrometers (Fig. 1(a)). To achieve the reparative reduction, the as-prepared GO films were rapidly inserted into a furnace in a flowing Ar/H<sub>2</sub> (200 sccm/100 sccm) gas mixture when its temperature reached 1000 °C. At the same time, a carbon source (5 sccm methane) was introduced for the whole reduction process, which lasted one hour. For the control experiment, GO film was thermally treated in the same way but without adding any carbon source.

After reparative reduction, (as shown in Fig. 1(b)), the film became smoother, which may be due to the removal of intercalated water between GO and the substrates, and a better contact between the layer and substrates resulting from treatment at high temperature. The sheet resistance of the single-layer reparatively reduced GO films was measured using a Loresta-EP MCP-T360 resistivity meter (Mitsubishi Chemicals) with 4-pin probes on silicon substrates with a 300 nm oxide layer. Reparative reduction resulted in an increase in the electrical conductivity of the films by more than 6 times to about 350–410 S/cm (Fig. 2(a)). This electrical conductivity is superior to previously reported results



**Figure 1** Tapping mode AFM height images of a GO sheet before (a) and after (b) the reparative reduction procedure

[10, 14], verifying that the recovery process has taken place. The rise in electrical conductivity suggests the extension of sp<sup>2</sup> islands and diminishment of the defect areas [11]. The sheet conductivity of multilayer graphene films (the film thickness was measured using an Ambios Technology XP-2 stylus profilometer) also increased after recovery (Fig. 2(b)). However, the magnitude of the increase was smaller than for the thin film. This results from the stacking of GO plates in the thicker film, which connects the dispersed pieces in a more dense state and weakens the effect of graphene basal-plane defects on electron transport. Consequently, this phenomenon confirms that the restored electrical conductivity mainly originates from the recovery of the aromatic structure by forming new bonds and repair of the defects. The optical transmission of the reparatively reduced films on quartz was measured in the range from 300 to 2500 cm<sup>-1</sup> using a Lambda 950 UV/vis spectrometer (PerkinElmer). There are obvious transmission differences between merely annealed and reparatively reduced GO films (Fig. 2(c)). The larger absorption in the latter suggests restoration of the  $\pi$ -electron system to a greater extent [10]. Notably, even with more aromatic regions restored, the graphene films still retain a high transmittance (more than 96%) over the visible and near infrared regions, which is acceptable for use in transparent conducting films. Table 1 shows a comparison of the optical transmission and electrical

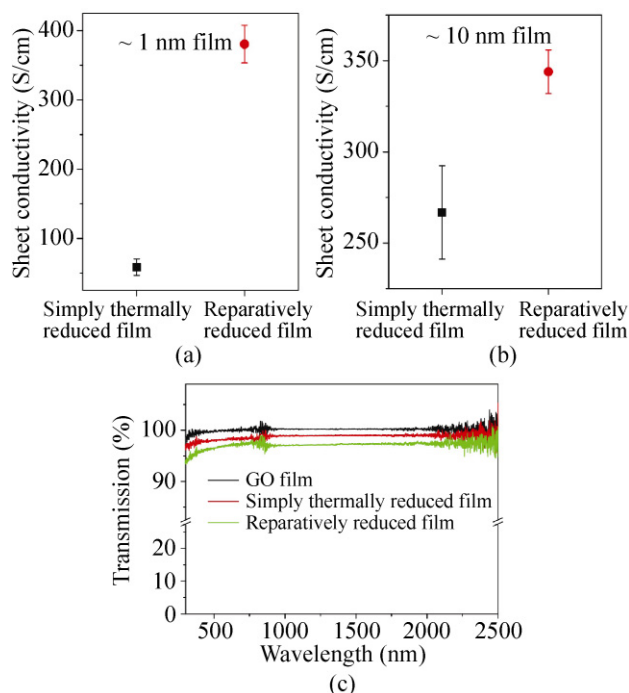


**Figure 2** (a), (b) Electrical conductivity of thermally reduced and reparatively reduced films on SiO<sub>2</sub>/Si and (c) optical transmission of the films on quartz

**Table 1** Performance comparison of r-GO films prepared by various reduction processes

Reduction process	Transparency (% @550 nm)	Sheet conductivity (S/cm)
1 <sup>a</sup> Hydrazine	90%	~0.01
2 <sup>b</sup> Hydrazine +400 °C	90%	10–100
3 <sup>c</sup> Electrical reduction	—*	~14
4 <sup>d</sup> CVD repair	—*	10–350
5 Thermal reduction	97%	52–64
6 Reparatively reduction	95%	350–410

a,b from Ref. [10]

c from Ref. [17]

d from Ref. [14]

\*Note: Transmittance data were not provided.

conductivity of various kinds of r-GO. Compared with chemically reduced GO [10], electrically reduced GO [17] and CVD-repaired GO [14], the high transparency and conductivity of our reparatively reduced films make them more competitive in transparent conductive applications.

X-ray photoelectron spectroscopy (XPS) was used to further investigate the recovery effect. As revealed in Figs. 3(a)–3(c), the increase in graphitic carbon (C–C,

about 284.4 eV) content shows that in the reparative reduction there is additional formation of C–C bonds. This is consistent with the observed decrease in the film resistance. Raman mapping using a micro-Raman spectrometer (633 nm excitation wavelength) was performed over an area of 100 μm<sup>2</sup> (1225 points in total) on the films to evaluate the repaired graphene films. As shown in Figs. 3(d)–3(g), both the wavenumber of the G peak and the D/G intensity ratio increased after the recovery process. A blue shift of the G peak is known to indicate sp<sup>2</sup> clustering and ordering. Meanwhile, the intensity ratio  $I(D)/I(G) \propto L_a^2$ , where  $L_a$  denotes the in-plane correlation length within an ordered graphite layer, i.e.,  $I(D)/I(G)$  is proportional to the number of aromatic rings [18]. Hence, the increased  $I(D)/I(G)$  ratio after the recovery process suggests the formation of sp<sup>2</sup> structures. Therefore, these results suggest that the recovery process we introduced during the thermal annealing procedure helps to decrease the number of oxygen-containing groups and to restore the aromatic structure of graphene basal plane.

During thermal annealing, the carbon source (CH<sub>4</sub>) decomposes into C<sub>x</sub> radicals [19], which can then react with the decomposed oxygen radicals to form stable carbon oxides, reducing the probability of vacancy-forming reactions by preventing oxygen radicals from carrying away the adjacent carbon atoms in the graphene basal plane; alternatively the carbon radicals can directly fill the vacancies formed and restore the six-membered aromatic rings through reaction with dangling bonds, just as in the recently reported process of “cloning” single-walled carbon nanotubes without a catalyst [20] (Scheme 1(c)). On this basis, it is important to make sure that the recovery and reduction of GO take place at the same time. However, GO begins to deoxygenize at 200 °C, which is too low a temperature to induce decomposition of the carbon source. Thus, a fast heating step and synchronous reduction and recovery are indispensable. Otherwise, using a normal heating process or a two-step increase, a number of vacancies will form without the opportunity to react with the carbon radicals and lose the chance of recovery.

In conclusion, we have established a facile method to obtain high-quality graphene films (with sheet



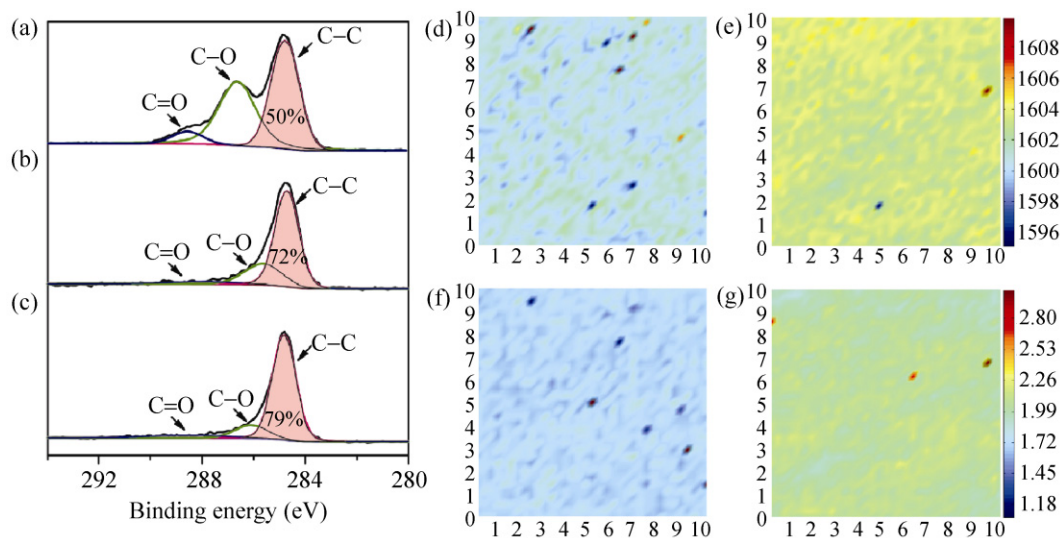


**Figure 3** XPS characterization of: GO (a); thermally reduced films (b); reparatively reduced films (c); raman mapping of the G peak position of thermally reduced films (d) and reparatively reduced films (e); D/G intensity ratio of thermally reduced films (f) and reparatively reduced films (g)

conductivity of ~350–410 S/cm and 96% transparency over the visible and near infrared range) via reparative reduction of GO. The restoration of the ordered graphene structure was realized by introducing carbon radicals when the vacancies with active ends were freshly generated. The easy scale-up of this one-step process could give chemically derived graphene a critical role in flexible and low-cost electronics, solar cells and optical devices as transparent electrodes. Moreover, the reparative reduction may provide an insight into the “cloning” of graphene, from peeled-off graphene to perfect large-area graphene.

## Acknowledgements

This work was supported by the National Natural Science Foundation of China (Grants Nos. 50802003, 20973013, 51072004, 50821061, and 20973006) and Ministry of Science and Technology of the people’s Republic of China (Grants Nos. 2007CB936203, 2006CBP32602, and 2009CB929403).

**Electronic Supplementary Material:** An AFM image of GO sheets and a Raman spectrum of reparatively reduced GO is available in the online version of this article at <http://dx.doi.org/10.1007/s12274-011-0099-8>.

## References

- Eda, G.; Fanchini, G.; Chhowalla, M. Large-area ultrathin films of reduced graphene oxide as a transparent and flexible electronic material. *Nat. Nanotechnol.* **2008**, *3*, 270–274.
- Stankovich, S.; Dikin, D. A.; Dommett, G. H. B.; Kohlhaas, K. M.; Zimney, E. J.; Stach, E. A.; Piner, R. D.; Nguyen, S. T.; Ruoff, R. S. Graphene-based composite materials. *Nature* **2006**, *442*, 282–286.
- Novoselov, K. S.; Geim, A. K.; Morozov, S. V.; Jiang, D.; Zhang, Y.; Dubonos, S. V.; Grigorieva, I. V.; Firsov, A. A. Electric field effect in atomically thin carbon films. *Science* **2004**, *306*, 666–669.
- Sutter, P. W.; Flege, J. I.; Sutter, E. A. Epitaxial graphene on ruthenium. *Nat. Mater.* **2008**, *7*, 406–411.
- Reina, A.; Jia, X. T.; Ho, J.; Nezich, D.; Son, H. B.; Bulovic, V.; Dresselhaus, M. S.; Kong, J. Large area, few-layer graphene films on arbitrary substrates by chemical vapor deposition. *Nano Lett.* **2009**, *9*, 30–35.
- Li, X. S.; Cai, W. W.; An, J. H.; Kim, S.; Nah, J.; Yang, D. X.; Piner, R.; Velamakanni, A.; Jung, I.; Tutuc, E.; Banerjee, S. K.; Colombo, L.; Ruoff, R. S. Large-area synthesis of high-quality and uniform graphene films on copper foils. *Science* **2009**, *324*, 1312–1314.
- Yang, X. Y.; Dou, X.; Rouhanipour, A.; Zhi, L. J.; Rader, H. J.; Mullen, K. Two-dimensional graphene nanoribbons. *J. Am. Chem. Soc.* **2008**, *130*, 4216–4217.

- [8] Li, X. L.; Zhang, G. Y.; Bai, X. D.; Sun, X. M.; Wang, X. R.; Wang, E.; Dai, H. J. Highly conducting graphene sheets and Langmuir–Blodgett films. *Nat. Nanotechnol.* **2008**, *3*, 538–542.
- [9] Li, D.; Muller, M. B.; Gilje, S.; Kaner, R. B.; Wallace, G. G. Processable aqueous dispersions of graphene nanosheets. *Nat. Nanotechnol.* **2008**, *3*, 101–105.
- [10] Becerril, H. A.; Mao, J.; Liu, Z.; Stoltenberg, R. M.; Bao, Z.; Chen, Y. Evaluation of solution-processed reduced graphene oxide films as transparent conductors. *ACS Nano* **2008**, *2*, 463–470.
- [11] Lerf, A.; He, H. Y.; Forster, M.; Klinowski, J. Structure of graphite oxide revisited. *J. Phys. Chem. B* **1998**, *102*, 4477–4482.
- [12] Gomez-Navarro, C.; Weitz, R. T.; Bittner, A. M.; Scolari, M.; Mews, A.; Burghard, M.; Kern, K. Electronic transport properties of individual chemically reduced graphene oxide sheets. *Nano Lett.* **2007**, *7*, 3499–3503.
- [13] Jung, I.; Dikin, D. A.; Piner, R. D.; Ruoff, R. S. Tunable electrical conductivity of individual graphene oxide sheets reduced at “low” temperatures. *Nano Lett.* **2008**, *8*, 4283–4287.
- [14] Lopez, V.; Sundaram, R. S.; Gomez-Navarro, C.; Olea, D.; Burghard, M.; Gomez-Herrero, J.; Zamora, F.; Kern, K. Chemical vapor deposition repair of graphene oxide: A route to highly conductive graphene monolayers. *Adv. Mater.* **2009**, *21*, 4683–4686.
- [15] Stankovich, S.; Piner, R. D.; Chen, X. Q.; Wu, N. Q.; Nguyen, S. T.; Ruoff, R. S. Stable aqueous dispersions of graphitic nanoplatelets via the reduction of exfoliated graphite oxide in the presence of poly(sodium 4-styrenesulfonate). *J. Mater. Chem.* **2006**, *16*, 155–158.
- [16] Hummers, W. S.; Offeman, R. E. Preparation of graphitic oxide. *J. Am. Chem. Soc.* **1958**, *80*, 1339–1339.
- [17] Liu, N.; Luo, F.; Wu, H. X.; Liu, Y. H.; Zhang, C.; Chen, J. One-step ionic-liquid-assisted electrochemical synthesis of ionic-liquid-functionalized graphene sheets directly from graphite. *Adv. Funct. Mater.* **2008**, *18*, 1518–1525.
- [18] Ferrari, A. C. Determination of bonding in diamond-like carbon by Raman spectroscopy. *Diamond Relat. Mater.* **2002**, *11*, 1053–1061.
- [19] Choudhary, T. V.; Aksoylu, E.; Goodman, D. W. Nonoxidative activation of methane. *Catal. Rev.—Sci. Eng.* **2003**, *45*, 151–203.
- [20] Yao, Y. G.; Feng, C. Q.; Zhang, J.; Liu, Z. F. “Cloning” of single-walled carbon nanotubes via open-end growth mechanism. *Nano Lett.* **2009**, *9*, 1673–1677.

